


Preparation of planar and hydrophobic benzocyclobutene-based dielectric material from biorenewable rosin

Fei Fu,^{1,2} Dan Wang,^{1,3} Minggu Shen ,^{1,3} Shibin Shang,^{1,3} Zhanqian Song,¹ Jie Song⁴

¹Institute of Chemical Industry of Forest Products, Chinese Academy of Forestry, Key Laboratory of Biomass Energy and Material, National Engineering Laboratory for Biomass Chemical Utilization, Key and Open Laboratory of Forest Chemical Engineering, State Forestry Administration, Nanjing, Jiangsu Province 210042, China

²Co-Innovation Center of Efficient Processing and Utilization of Forest Resources, Nanjing Forestry University, Nanjing 210037, People's Republic of China

³Institute of New Technology of Forestry, Chinese Academy of Forestry, Beijing 100091, China

⁴Department of Chemistry and Biochemistry, University of Michigan-Flint, Flint, Michigan 48502

Correspondence to: M. Shen (E-mail: mingguishen@163.com) and Z. Song (E-mail: songzq@hotmail.com)

ABSTRACT: A rosin-based monomer with thermally crosslinkable benzocyclobutene groups was synthesized in this study. The structure of the monomer was examined using mass spectroscopy, Fourier transform infrared spectroscopy, and nuclear magnetic resonance spectroscopy. An amorphous crosslinked network with dielectric constant of 2.71 and dielectric loss of 0.0012 at 30 MHz was formed when the monomer was polymerized at high temperature (> 200 °C). The polymer film exhibits surface roughness (Ra) of 0.337 nm in a 5.0 × 5.0 μm² area and the water contact angle of 110°. In addition, results from thermogravimetric analysis indicate that the polymer has T_{5%} = 402 °C, and differential scanning calorimetry measurements show that the glass transition temperature is at least 350 °C. Results from nanoindentation tests show that the hardness and Young's modulus of the polymer are 0.418 and 4.728 GPa, respectively. These data suggest that this new polymer may have potential applications in electronics and microelectronics. © 2019 Wiley Periodicals, Inc. *J. Appl. Polym. Sci.* **2020**, *137*, 48831.

KEYWORDS: biomaterials; dielectric properties; thermosets

Received 28 August 2019; accepted 28 November 2019

DOI: 10.1002/app.48831

INTRODUCTION

With the development of microelectronics, the sizes of individual devices have become progressively smaller. Scaling down generates problems such as interconnect signal delay (RC delay) that gives rise to propagation delay, crosstalk noise, and power dissipation.^{1–4} These problems have become an obstacle to further development within the microelectronics. The use of interconnect materials with low dielectric constant is one effective way to reduce RC delay.^{5–8} Therefore, the development of materials with low dielectric constant has received widespread attention.^{1–8} One method for decreasing the dielectric constant is to prepare porous materials because the dielectric constant of air is approximately 1. However, high porosity will decrease the mechanical strength and increase water absorption, thus increasing the dielectric constant.² Additionally, Long *et al.* synthesized polymers using ring-opening olefin metathesis polymerization of strained cyclic olefinic monomers.⁹ The material was found to

have a low dielectric constant from free volume theory. An alternative method is to use intrinsically low-k polymers, such as SiLK, poly(benzoxazole)s, and polyimides.^{10–13} Among these, benzocyclobutene (BCB) resins, as one family of low-k polymers, have attracted much attention in recent years.^{14–17} The monomer BCB could exhibit a ring-opening reaction in certain circumstances, yielding a cured resin.^{14,16–23} No catalyst is required and no volatile compounds are released during the curing process. Generally, the resulting BCB resins show excellent dielectric properties and thermal stability, low water absorption and thermal expansion coefficient.²⁴ Correspondingly, BCB resins have been widely used in aerospace, electronics and microelectronics, in applications such as enameled wire varnish, large-scale integrated circuits, and composite materials.^{25–27}

The development of biobased polymers is promoted by growing concerns of long-term sustainability and the negative environmental footprint of petroleum-based polymer materials.^{28–33}

Additional Supporting Information may be found in the online version of this article.

© 2019 Wiley Periodicals, Inc.

Rosin acid is renewable, biodegradable, and biocompatible, and it has a large hydrogenated phenanthrene ring structure, thus it could be used to synthesize and modify polymer materials.³⁴ However, rosin containing conjugated double bonds can easily react with oxygen, which decreases the material quality, so methods including hydrogenation, disproportionation, and polymerization are needed to modify rosin to improve its stability.³⁵

Rosin derivatives may serve as alternatives to petroleum-based aromatic compounds or cycloaliphatic compounds that are generally used to modify polymers and improve their thermal and mechanical properties.³⁶ The hydrogenated phenanthrene ring, as a characteristic functional group of rosin, significantly affects the hydrophobic and thermomechanical properties of polymers.^{37–45}

Moreover, as the primary structural unit of target polymer, the huge hydrogenated phenanthrene ring structure can effectively block the winding of molecular segments, which increases the intermolecular spacing and free volume in polymer molecules.^{46,47} Therefore, the introduction of the hydrogenated phenanthrene ring might yield the BCB resins with good hydrophobic, thermomechanical, and dielectric properties.

In this study, a new rosin-based monomer containing bibenzocyclobutene groups was synthesized using dehydroabietic acid (DA) as the raw material. The monomer synthesis route and monomer molecular structure are shown in Scheme 1. After ring-opening polymerization at high temperature, a crosslinked network was formed in the monomer, providing good hydrophobic, mechanical, and dielectric properties. These results indicate that the polymer is suitable as an encapsulation resin or dielectric material in electronics and microelectronics. Overall,

the exhibited properties are comparable with other reported BCB-based dielectric materials, while at the same time, this work is a good exploration for the application of biobased materials in different areas.

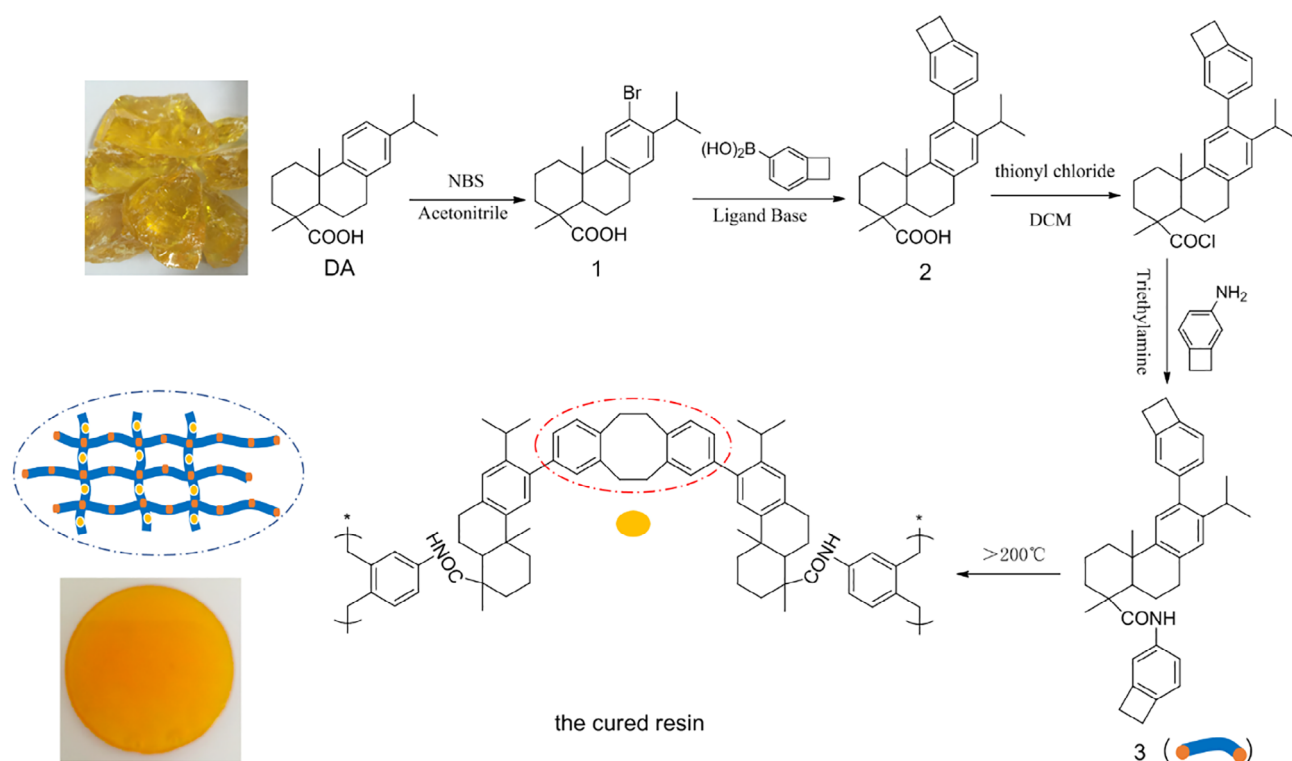
EXPERIMENTAL SECTION

Materials

Benzocyclobutene-4-boronic acid and 4-aminobenzocyclobutene were purchased from Chemtarget Technologies Co., Ltd. DA was obtained from Wuzhou chemical Co., Ltd. *N*-Bromosuccinimide (NBS), tripotassium phosphate, triethylamine, thionyl chloride, and tetrakis(triphenylphosphine)palladium (0) were obtained from Aladdin Industrial Corporation. Ethanol, acetonitrile, mesitylene, dichloromethane, ethyl acetate, and petroleum ether were purchased from Nanjing Chemical Reagent Co., Ltd. All chemicals were used without purification.

Measurements

¹H and ¹³C nuclear magnetic resonance (NMR) spectra were recorded at room temperature with a spectrometer (Bruker 400) using TMS as an internal standard with DMSO as a solvent. Fourier transform infrared (FTIR) spectra were gathered with a Thermo Scientific Nicolet IS10 spectrometer (Nicolet) using attenuated total reflectance measurements. Mass spectra from the compounds were recorded with a Waters Q-TOF Micro mass spectrometer (MS). Thermogravimetric analysis (TGA) was performed with a TG209F1 (NETZSCH, Germany) apparatus at a heating rate of 10 °C min⁻¹ in N₂ atmosphere. Differential scanning calorimetry (DSC) measurements were gathered with a Perkin Elmer Diamond Differential Scanning Calorimeter a



Scheme 1. Procedure for the synthesis of new monomer and cured resin. [Color figure can be viewed at wileyonlinelibrary.com]

heating rate of 10 °C min⁻¹ in N₂ atmosphere. The contact angle of the cured resin was measured at room temperature with a dynamic contact angle measurement instrument (JC2000C) using the sessile drop method. Deionized water was used as the testing liquid. The surface toughness of the polymer film was measured using an atomic force microscope (AFM Shimadzu SPM-9600, Japan). The dielectric constant (ϵ') and dielectric loss ($\tan \delta$) of the cured resin were measured at frequencies ranging from 1.0 to 30 MHz at room temperature using a 4294A Precision Impedance Analyzer (Agilent). The mechanical properties of the cured resin were measured with a nanoindentation system (UNHT, Anton Paar). The phase structure of as-prepared product was characterized with X-ray diffraction (XRD, Bruker D8 advance with Cu K α). The scans were taken within the 2 θ range between 5 and 40° and operated at an accelerating voltage of 40 kV and an emission current of 40 mA.

Synthesis of Compound 1

DA (0.017 mol, 5.00 g) was dissolved in anhydrous acetonitrile (337 mL), and NBS (0.031 mol, 5.54 g) was added. The mixture was allowed to react in darkness at room temperature for 24 h. The mixture was suction filtered, yielding a white solid that was dissolved in ethyl acetate (50 mL). Then, the organic phase was washed with water (three times with 50 mL) and dried over anhydrous Na₂SO₄. After filtration and concentration, Compound 1 was purified using column chromatography with a mixture of petroleum ether and ethyl acetate as the eluent (5:1, v/v). Yield: 53%. ¹H NMR (400 MHz, DMSO) δ 12.20 (s, 1H), 7.36 (s, 1H), 7.00 (s, 1H). ¹³C NMR (101 MHz, DMSO) δ 179.2 (m), 149.2 (s), 143.2 (s), 134.5 (s), 128.0 (s), 127.2 (s), 120.8 (m), 46.2 (s), 44.2 (s), 37.5 (s), 36.5 (s), 36.1 (s), 31.9 (s), 28.9 (s), 24.6 (s), 22.7 (s), 22.6 (s), 20.8 (m), 18.0 (s), 16.3 (s); MS (ESI) m/z 377 [M - H]⁻.

Synthesis of Compound 2

Compound 1 (1.00 mmol, 0.379 g), tripotassium phosphate (2.00 mmol, 0.425 g), and benzocyclobutene-4-boronic acid (1.25 mmol, 0.185 g) were dissolved in a water/ethanol mixture (6 mL, 1:1, v/v) in a N₂ atmosphere. Tetrakis(triphenylphosphine) palladium (0) (0.01 mmol, 0.0116 g) was added, and the mixture was subsequently heated at 60 °C for 10 h. The mixture was allowed to cool to room temperature and suction filtered with diatomite. The filtrate then was extracted with ethyl acetate (two times with 30 mL). The organic phases were combined, washed with water (three times with 50 mL), dried over anhydrous Na₂SO₄, filtered, and concentrated to yield the crude product. Compound 2 was purified using column chromatography with a mixture of petroleum ether and ethyl acetate as the eluent (5:1, v/v). Yield: 85%. ¹H NMR (400 MHz, DMSO) δ 12.16 (s, 1H), 7.10 (d, J = 7.5 Hz, 1H), 7.02 (dd, J = 7.5, 0.9 Hz, 1H), 7.00 (s, 1H), 6.93 (s, 1H), 6.91 (s, 1H), 3.18 (s, 4H). ¹³C NMR (101 MHz, DMSO) δ 179.4 (s), 146.27 (s), 144.9 (s), 143.4 (s), 142.5 (s), 140.6 (s), 138.9 (s), 133.5 (s), 127.7 (s), 125.4 (s), 125.3 (s), 123.2 (s), 122.0 (s), 46.3 (s), 44.6 (s), 37.7 (s), 36.3 (s), 36.2 (s), 29.2 (s), 29.0 (s), 28.9 (s), 28.3 (s), 24.8 (s), 24.2 (s), 24.0 (s), 21.1 (s), 18.1 (s), 16.3 (s); MS (ESI) m/z 401 [M - H]⁻.

Synthesis of Monomer 3

Compound 2 (4.97 mmol, 2.00 g) was dissolved in dichloromethane (15 mL). Thionyl chloride (9.94 mmol, 1.18 g) was added slowly. After the solution was heated to reflux while stirring for 4.0 h, excessive thionyl chloride was removed by distillation, yielding the reaction crude. 4-aminobenzocyclobutene (5.96 mmol, 0.71 g) was dissolved in dichloromethane (15 mL), and triethylamine (14.91 mmol, 1.51 g) was added. The crude was dissolved in dichloromethane (5.0 mL), and the solution was added dropwise at room temperature. The mixture was stirred for 12 h at room temperature, and 10% HCl (20 mL) was added to annihilate. Then, the water phase was extracted with ethyl acetate (two times with 30 mL). The organic phases were combined, washed with water (3 times with 50 mL), dried over anhydrous Na₂SO₄, filtered, and concentrated to yield the crude product. Monomer 3 was purified using column chromatography with a mixture of petroleum ether and ethyl acetate as the eluent (5:1, v/v). Yield: 92%. ¹H NMR (400 MHz, DMSO) δ 9.20 (s, 1H), 7.39 (s, 1H), 7.29 (d, J = 7.9 Hz, 1H), 7.10 (d, J = 7.4 Hz, 1H), 7.02 (s, 1H), 7.00 (s, 1H), 6.97 (d, J = 8.3 Hz, 1H), 6.95 (s, 1H), 6.92 (s, 1H), 3.17 (s, 4H), 3.07 (s, 4H). ¹³C NMR (101 MHz, DMSO) δ 176.3 (s), 146.7 (s), 144.9 (s), 144.8 (s), 143.5 (s), 142.5 (s), 140.6 (s), 139.9 (s), 138.9 (s), 138.2 (s), 133.8 (s), 127.7 (s), 125.4 (s), 125.3 (s), 123.1 (s), 122.3 (s), 122.0 (s), 120.0 (s), 116.0 (s), 47.4 (s), 44.2 (s), 37.2 (s), 36.7 (s), 35.8 (s), 29.2 (s), 29.1 (s), 28.9 (s), 28.7 (s), 28.6 (s), 28.4 (s), 24.9 (s), 24.3 (s), 23.9 (s), 20.6 (s), 18.5 (s), 16.3 (s); MS (ESI) m/z 526 [M + Na]⁺.

Preparation of BCB Polymers

The rosin-based BCB resin was prepared by placing Monomer 3 directly into a glass mold. After degassing in a vacuum oven at 160 °C for 1.0 h, the mold was heated stepwise at 180 °C for 1.0 h, 200 °C for 4.0 h, 210 °C for 4.0 h, 230 °C for 4 h, 250 °C for 6 h, and 270 °C for 1.0 h (under nitrogen atmosphere). The cured sample was used to measure the dielectric properties and for nanoindentation tests.

Monomer 3 (100 mg) was dissolved in mesitylene (1.0 mL) and refluxed for 10 h to obtain oligomers. The oligomer was spin-coated on a silicon wafer to form a smooth film, which was dried for 24 h at room temperature in a vacuum oven. The silicon wafer was placed in a tube furnace and heated stepwise at 180 °C for 1.0 h, 200 °C for 4.0 h, 210 °C for 4.0 h, 230 °C for 4 h, 250 °C for 6 h, and 270 °C for 1.0 h. After allowing the wafer to cool to room temperature, the sample was used to measure the surface toughness of the film.

RESULTS AND DISCUSSION

Synthesis and Characterization

Monomer 3 was prepared via three steps using DA as the feedstock as shown in Scheme 1. DA was reacted to obtain a brominated intermediate (Compound 1), which was then reacted with benzocyclobutene-4-boronic acid to afford Compound 2 via a Suzuki coupling reaction. Taking the carboxyl group as the active site, Compound 2 was then reacted with 4-aminobenzocyclobutene to yield a rosin monomer with two BCB groups (Monomer 3) via an amide reaction. The chemical structures of the compounds were confirmed by ¹H NMR, ¹³C NMR, and MS measurements (see in

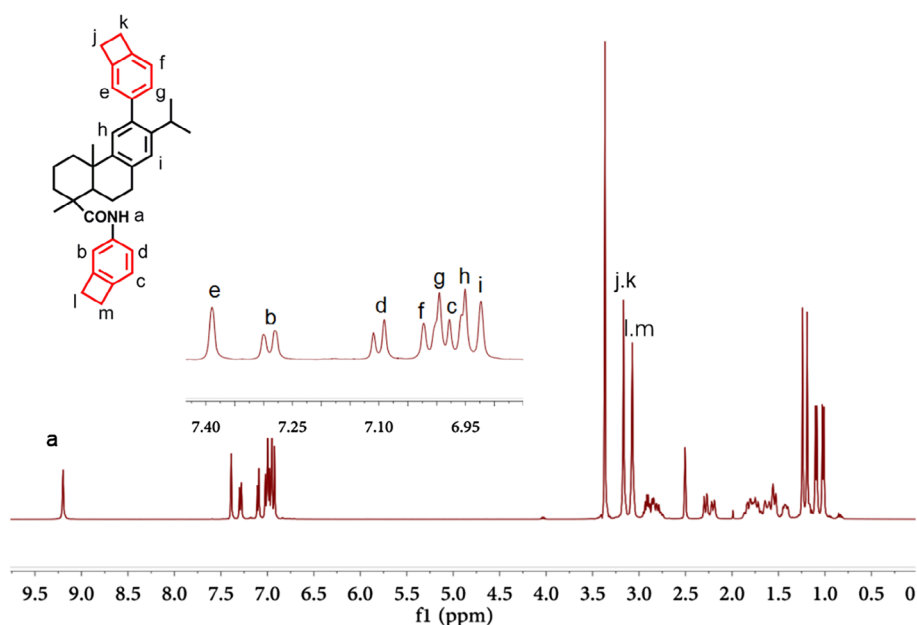


Figure 1. ^1H NMR spectra of Monomer 3. [Color figure can be viewed at wileyonlinelibrary.com]

Supporting Information). Under elevated temperature, there is no difference in reactivity between the two BCB groups. Moreover, coupling to form an 8-member ring and ring-opening polymerization are both possible. Scheme 1 illustrated one kind of the structure of the polymer.

The chemical structure of Monomer 3 was characterized by ^1H NMR, ^{13}C NMR, and FTIR spectra (Figures 1–3). One can see from Figure 1 that the peak at 9.20 ppm derives from proton in the $-\text{CONH}-$ groups; the peaks at 7.39–6.92 ppm are attributed to protons in the benzene ring; the characteristic peaks from the protons on the four-membered ring of BCB

appear at 3.17 and 3.07 ppm, and the signals from 3.0 to 0.5 ppm are assigned to protons attached to the hydrogenated phenanthrene ring.⁴⁸ The peak at 176.3 ppm in the ^{13}C NMR spectrum (Figure 2) belongs to carbon atom in the amide group; the peaks from carbon atoms in the benzene ring appear at 146.7, 144.9, 144.8, 143.5, 142.5, 140.6, 139.9, 138.9, 138.2, 133.8, 127.7, 125.4, 125.3, 123.1, 122.3, 122.0, 120.0, and 116.0 ppm; the signals from carbon atoms in cyclobutene are located at 29.1, 28.9, 28.7, and 28.6 ppm, and the remaining peaks are attributed to carbon atoms in the hydrogenated phenanthrene ring. FTIR spectra from Monomer 3 are shown in

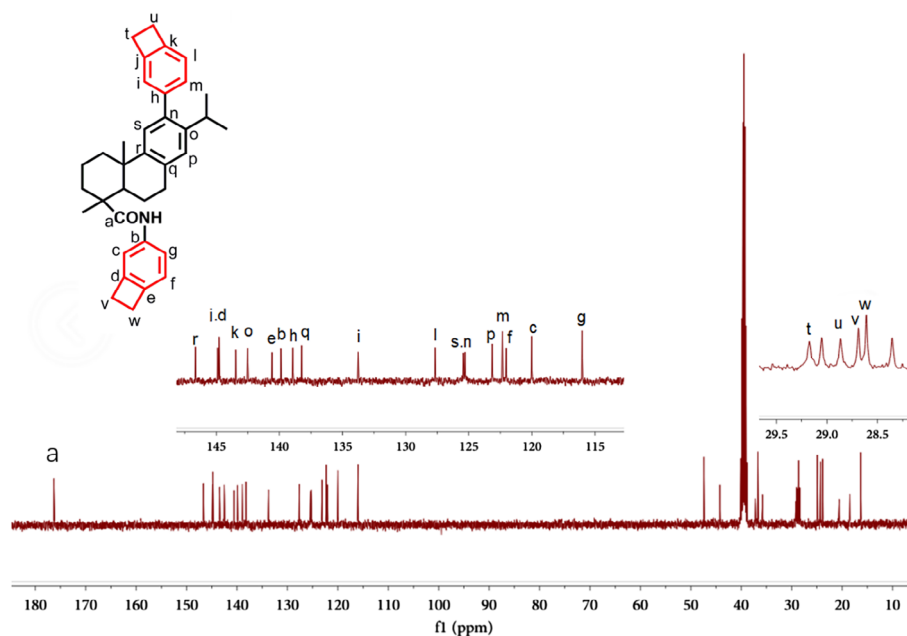


Figure 2. ^{13}C NMR spectra of Monomer 3. [Color figure can be viewed at wileyonlinelibrary.com]

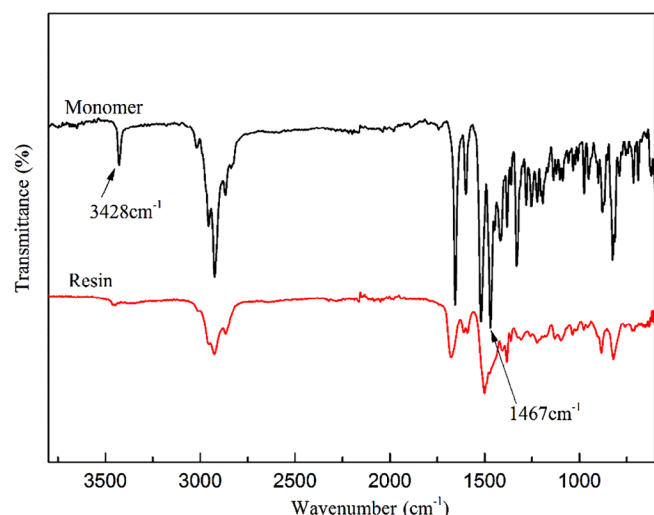


Figure 3. FTIR spectra of Monomer 3 and resin. [Color figure can be viewed at wileyonlinelibrary.com]

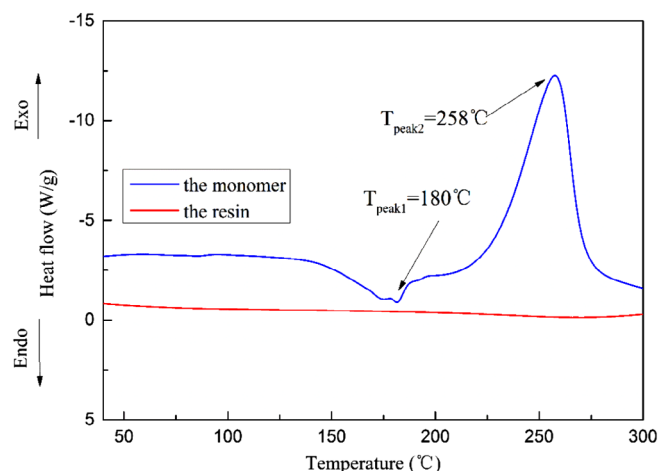


Figure 4. DSC curves of Monomer 3 and resin gathered at a heating rate of $10\text{ }^{\circ}\text{C min}^{-1}$. [Color figure can be viewed at wileyonlinelibrary.com]

Figure 3. The peak at 3428 cm^{-1} belongs to the N–H stretching vibration, and the absorption peak at 1467 cm^{-1} is ascribed to the in-plane ring stretching vibration of C–H in the four-member ring

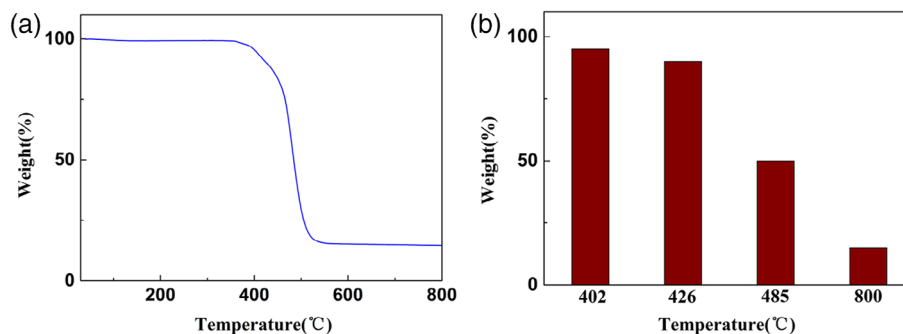


Figure 5. Thermal stability of the cured resin: (a) TG curve and (b) the residual yield of the resin at each temperature. [Color figure can be viewed at wileyonlinelibrary.com]

of BCB group.⁴⁹ Thus, all data are consistent with the chemical structure of Monomer 3.

Curing Behavior

The curing behavior of Monomer 3 was characterized using DSC, and the result is shown in Figure 4. The endothermic peak indicates melting at $180\text{ }^{\circ}\text{C}$. An exothermic peak is observed when the temperature increases above $200\text{ }^{\circ}\text{C}$, which is attributed to a ring-opening reaction in BCB units. Moreover, the exothermic peak temperature $T_{\text{max}} = 258\text{ }^{\circ}\text{C}$. The curing behavior of the monomer is similar that observed in BCB containing compounds.³³ The polymerization degree of the monomer was estimated from the DSC trace. After the resin was heated from 40 to $300\text{ }^{\circ}\text{C}$ at $10\text{ }^{\circ}\text{C min}^{-1}$ in N_2 , the DSC trace shows that no exothermic peak is observed, indicating complete polymerization.²⁷

The progress of the curing reaction of Monomer 3 was examined using FTIR spectroscopy. FTIR spectra for from monomer and the cured resin are shown in Figure 3. The characteristic peaks for the BCB group at 1467 cm^{-1} disappear after the curing reaction. Moreover, the characteristic peak of BCB monomers at 1467 cm^{-1} is transferred to 1500 cm^{-1} after the polymerization.⁴⁶ This result suggests that the monomer has been fully converted to a cured resin.

Thermal Stability

The thermostability of the cured resin was investigated using TGA. Figure 5(a) shows a TGA curve from the cured resin when heated at $10\text{ }^{\circ}\text{C min}^{-1}$ in N_2 . The $T_{5\%}$ value is chosen as a measure of thermal stability, which represents the temperature at 5% mass loss. As shown in Figure 5(b), $T_{5\%}$, $T_{10\%}$, and $T_{50\%}$ of the cured resin are 402 , 426 , and $485\text{ }^{\circ}\text{C}$, respectively; the residual yield of the cure resin is 14.6% at $800\text{ }^{\circ}\text{C}$. It is known that the structural unit of the polymer is primarily composed of rigid benzene ring and hydrogenated phenanthrene ring, so such high thermal stability may result from the planar structure of either the phenanthrene or phenyl rings that give room for ordered packing of the rigid structures.⁴⁰ Additionally, the BCB groups can be used as the crosslinking unit during curing. It is well known that the crosslinking structure can effectively improve the thermal stability of polymers.³⁶ Moreover, the glass transition temperature (T_g) of the cured resin was investigated using DSC. Figure 6 shows the T_g value of the cured resin when heating at

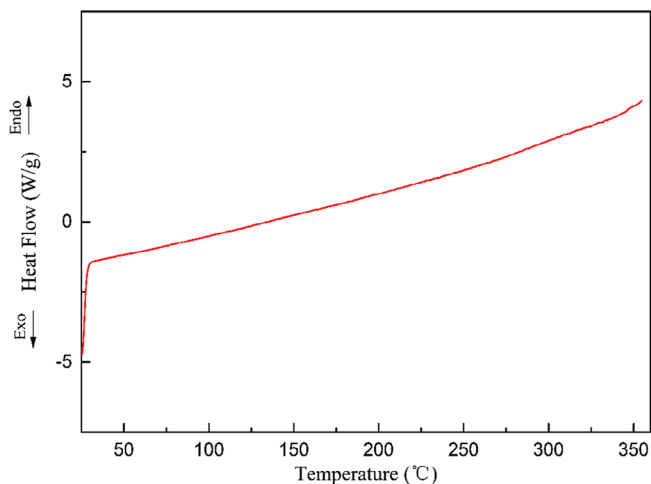


Figure 6. DSC curve of the cured resin. [Color figure can be viewed at wileyonlinelibrary.com]

10 °C min⁻¹ in N₂. The DSC trace indicates no evidence of a glass transition at temperatures ranging from 50 to 350 °C.

Mechanical Properties

The mechanical properties of the cured resin were determined using a nanoindentation system. The hardness and Young's modulus of the polymer were calculated from a force vs indentation

depth curve. Young's modulus can be calculated using eq. (1)⁵⁰⁻⁵²:

$$\frac{1}{E_r} = \frac{1-\nu}{E} + \frac{1-\nu_i}{E_i} \quad (1)$$

where E_i and ν_i are the Young's modulus (1141 GPa) and Poisson's ratio (0.07) of a diamond indenter, E_r is the reduced elastic modulus, and E and ν are the Young's modulus and Poisson's ratio of the sample, respectively. We used $\nu = 0.34$ for polymer materials.⁵³ The sample's hardness (H) can be determined by dividing the peak load (P_{\max}) by contact area (A), eq. (2)⁵⁰⁻⁵²:

$$H = \frac{P_{\max}}{A} \quad (2)$$

The results of the four tests are shown in Figure 7. As shown in Figure 7(a), the pressure and indentation depth curves nearly overlap. Moreover, the values of hardness and Young's modulus for the resin are similar [Figure 7(b,c)]. The results show that the cured resin has an average hardness of 0.418 GPa and a Young's modulus of 4.728 GPa. Some researchers have noted that the introduction of a hydrogenated phenanthrene ring effectively improves the mechanical properties of polymer (e.g., silicone rubber, polylactic acid, and epoxy resin).^{36,42,54} Therefore, the introduction of a hydrogenated phenanthrene ring improves the mechanical properties of the polymer, and the polymer has a crosslinked structure, so the polymer has excellent mechanical properties.

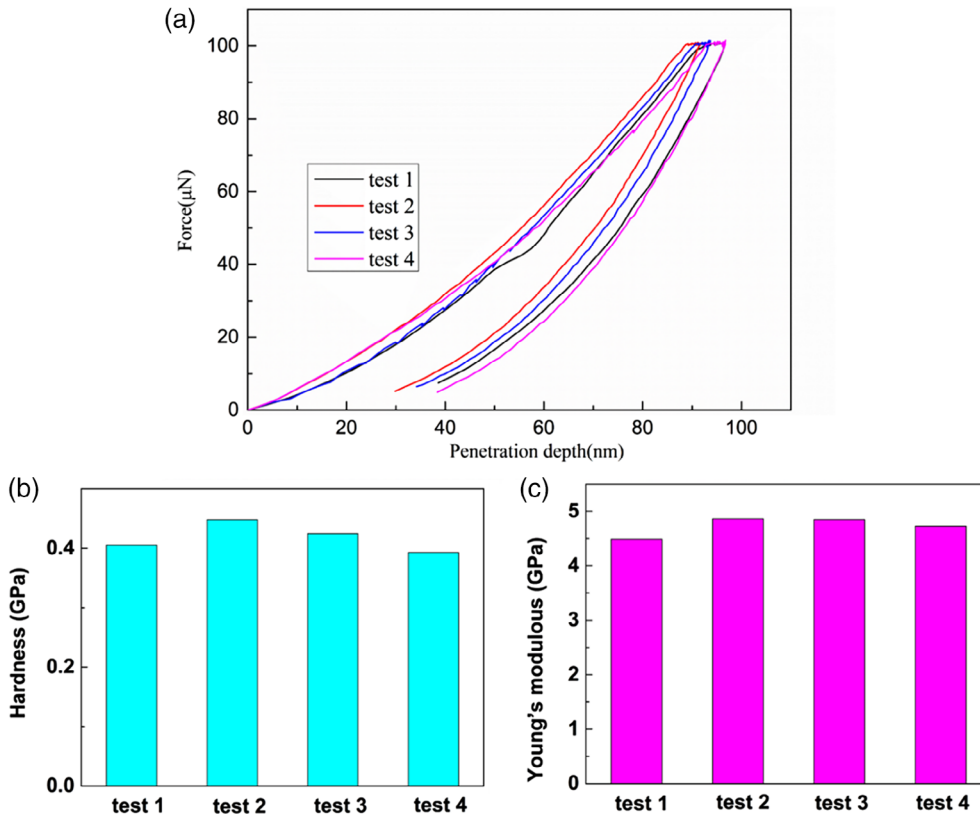


Figure 7. Results from nanoindentation tests for the cured resin: (a) pressure vs indentation depth curves, (b) hardness, and (c) Young's modulus of the resin. [Color figure can be viewed at wileyonlinelibrary.com]

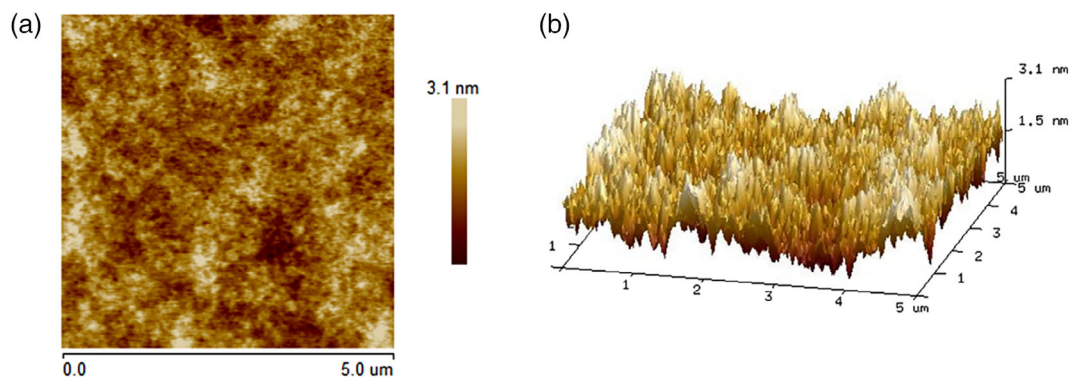


Figure 8. AFM images of the cured resin film: (a) planar graph and (b) stereogram. [Color figure can be viewed at wileyonlinelibrary.com]

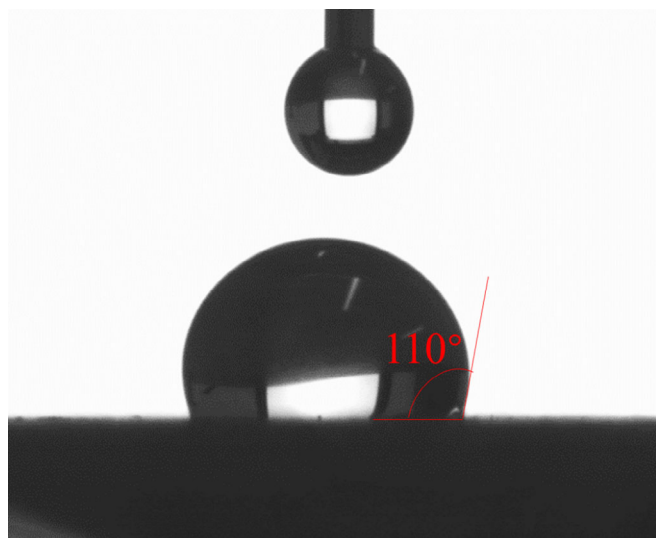


Figure 9. Contact angle of water on the cured resin. [Color figure can be viewed at wileyonlinelibrary.com]

Surface Roughness

The surface roughness of the polymer cast on a silicon wafer was investigated using an AFM. Both planar graph and stereogram are shown in Figure 8. The difference between the maximum and minimum thickness is 3.1 nm. Moreover, the measurements show that the average surface roughness (Ra) of the cured resin is 0.337 nm within a $5.0 \times 5.0 \mu\text{m}^2$ area, and the Ra value of cured resin could be comparable to the reported BCB resins, such as fluorinated BCB resins,²⁷ siloxane-based BCB resins,² and BCB resins containing bulk groups.⁴⁶ It is well known that the BCB-based resin exhibits good surface roughness,^{27,33,46} and the introduction of rosin did not affect the surface smoothness of the resin. We think rosin and BCB are both rigid structures, so they have a certain degree of compatibility. Therefore, there is no obvious shrinkage or expansion during curing of the rosin-based BCB monomer. In addition, the surface roughness is more important for the materials utilized in electronics and microelectronics, because low surface roughness implies that an array with high quality can be easily produced on the film surface.³³

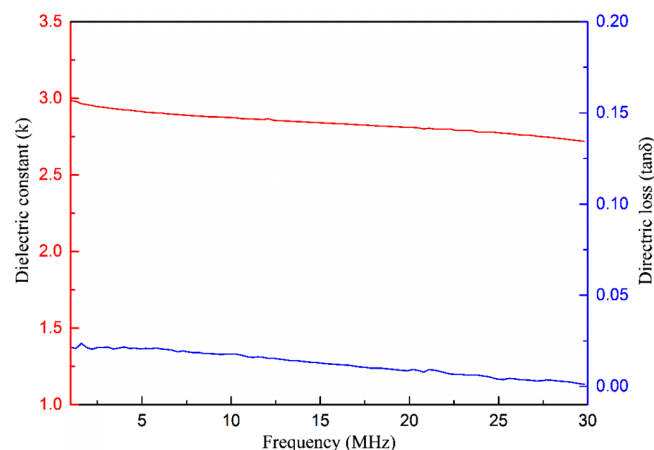


Figure 10. Dielectric constant and dielectric loss of the cured resin. [Color figure can be viewed at wileyonlinelibrary.com]

Hydrophobic Property

Hydrophobicity is a more important parameter for the application of high-performance material in the electronics and microelectronics, because it governs moisture adsorption and deterioration of dielectric properties.²⁷ The hydrophobicity of the cured resin was investigated using contact angle tests with deionized water. The water contact angle is found to be 110° (Figure 9). It is noted that the water contact angle of cured resin is better than the reported BCB resins, such as 96° ,³³ 102° ,²⁷ and 107° .⁴⁶ Additionally, a resin disk with a thickness of 2.0 mm and a diameter of 12.0 mm was kept in boiling water for 2 days, exhibiting a water uptake of 0.32%. The result indicates the resin has good hydrophobicity because of the introduction of rosin acid. As a hydrophobic group, the introduction of the hydrogenated phenanthrene ring can improve the hydrophobicity of polymeric materials.^{44,45} Moreover, the polymer structure has a slightly flexible chain segment, and the rigid structure will improve the hydrophobicity of polymer.⁴⁴

Dielectric Properties

Dielectric properties are also important parameters for materials applied in electronics packaging. The dielectric properties of the cured resin were measured using the capacitance method, and the results are shown in Figure 10. Electromagnetic waves propagate with a higher velocity when dielectric constant is lower,

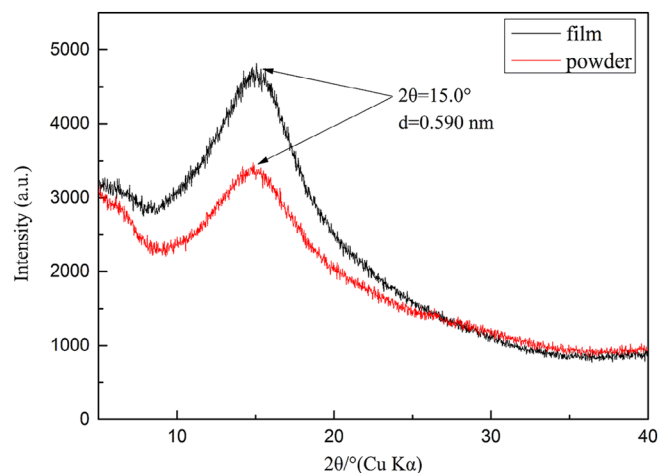


Figure 11. X-ray diffraction patterns of the cured resin (film and powder). [Color figure can be viewed at wileyonlinelibrary.com]

leading to lower line capacitance per unit length and higher characteristic impedance for a fixed conductor cross section.⁴⁶ Figure 10 shows the cured resin dielectric constant (k) of 2.71 and dielectric loss ($\tan \delta$) of 0.0012 at 30 MHz. Moreover, the average k value of 2.84 and $\tan \delta$ of 0.012 frequencies ranging from 1.0 to 30 MHz at room temperature. One should note that the k value of the cured resin is comparable to the commercially available organic low- k materials, such as polyimides (3.1–3.4),^{11,12} SILK resins (2.65),¹⁰ and polycyanate esters (2.61–3.12).⁵⁵

The good dielectric property of the cured resin can be explained by the Debye equation, as shown in eq. (3)⁸:

$$\frac{k-1}{k+2} = \frac{4\pi}{3} N \left(\alpha_e + \alpha_d + \frac{\mu}{3k_b T} \right) \quad (3)$$

where k is the dielectric constant, N is the number density of dipoles, α_e is the electric polarization, α_d is the distortion polarization, μ is the orientation polarization related to the dipole moment, k_b is the Boltzmann's constant, and T is the temperature. The rosin structure is primarily composed of C–C bonds, so the introduction of rosin can decrease the electron density and make the molecule difficult to polarize, thus decreasing α_d and α_e .⁴⁶ Additionally, the bulky hydrogenated phenanthrene ring structure moieties prevent molecular stacking and increase the free volume of the polymer, thus diminishing N and μ .^{8,46} The reduction of all the factors (α_d , α_e , N , and μ) in eq. (3) indicates that the resin has good dielectric property.

The XRD patterns in Figure 11 indicate that the cured resin is essentially amorphous and molecular stacking is prevented. The XRD peak at $2\theta = 15.0^\circ$ corresponds to a d value of 0.590 nm in the cured resin. Such large d spacing confirms the existence of a large free volume in the polymer, so the cured resin exhibits low- k value.⁷

CONCLUSION

In summary, a rosin-based dibenzocyclobutene polymerizable monomer was designed and successfully synthesized. A crosslinked network was formed after polymerization, and the polymerized

material exhibited an average dielectric constant of 2.84 and dielectric loss of 0.012 frequencies ranging from 1.0 to 30 MHz at room temperature. The cured resin had good thermal ability with $T_{5\%}$ of 402 °C and no glass transition at temperature below 350 °C. In addition, the cured resin showed excellent film uniformity and good hydrophobicity with the surface roughness (R_a) of 0.337 nm in a $5.0 \times 5.0 \mu\text{m}^2$ area and the water contact angle of 110°. The cured resin possessed good mechanical properties, with hardness, Young's modulus of 0.418, 4.728 GPa, respectively. These results indicate that the thermosetting polymer derived from rosin acid is suitable for use in electronics and microelectronics.

ACKNOWLEDGMENTS

The authors express their gratitude for the financial support provided by the Fundamental Research Funds of CAF (CAFYBB2017SY035), Natural Science Foundation of Jiangsu Province of China (BK20150071), and National Science Foundation of China (31500487).

CONFLICT OF INTEREST

The authors declare no conflict of interest.

REFERENCES

- Huang, Y.; Zhang, S.; Hu, H.; Wei, X.; Yu, H.; Yang, J. *Polym. Adv. Technol.* **2017**, *28*, 1480.
- Cheng, Y.; Chen, W.; Li, Z.; Zhu, T.; Zhang, Z.; Jin, Y. *RSC Adv.* **2017**, *7*, 14406.
- Zhang, S.; Hu, H.; Yu, H.; Huang, Y.; Yang, J. *Macromol. Res.* **2017**, *25*, 381.
- He, F.; Jin, K.; Wang, J.; Luo, Y.; Sun, J.; Fang, Q. *Macromol. Chem. Phys.* **2015**, *216*, 2302.
- Huang, Y.; Zhang, S.; Hu, H.; Wei, X.; Yu, H.; Yang, J. *J. Polym. Sci., Part A: Polym. Chem.* **2017**, *55*, 1920.
- Zhao, B.; Zhao, C.; Wang, C.; Park, C. B. *J. Mater. Chem. C.* **2018**, *6*, 3065.
- Yuan, C.; Wang, J.; Jin, K.; Diao, S.; Sun, J.; Tong, J.; Fang, Q. *Macromolecules.* **2014**, *47*, 6311.
- Yuan, C.; Jin, K.; Li, K.; Diao, S.; Tong, J.; Fang, Q. *Adv. Mater.* **2013**, *25*, 4875.
- Long, T. M.; Swager, T. M. *J. Am. Chem. Soc.* **2003**, *125*, 14113.
- Martin, S. J.; Godschalx, J. P.; Mills, M. E.; Ii, E. O. S.; Townsend, P. H. *Adv. Mater.* **2000**, *12*, 1769.
- Maier, G. *Prog. Polym. Sci.* **2001**, *26*, 3.
- Watanabe, Y.; Shibasaki, Y.; Ando, S.; Ueda, M. *Polym. J.* **2006**, *38*, 79.
- Volkens, W.; Miller, R. D.; Dubois, G. *Chem. Rev.* **2010**, *110*, 56.
- Tong, J.; Diao, S.; Jin, K.; Yuan, C.; Wang, J.; Sun, J.; Fang, Q. *Polymer.* **2014**, *55*, 3628.
- Cheng, Y.; Yang, J.; Jin, Y.; Deng, D.; Xiao, F. *Macromolecules.* **2012**, *45*, 4085.

16. Cao, K.; Yang, L.; Huang, Y.; Chang, G.; Yang, J. *Polymer*. **2014**, *55*, 5680.
17. Tan, L. S.; Venkatasubramanian, N.; Mather, P. T.; Houtz, M. D.; Benner, C. L. *J. Polym. Sci., Part A: Polym. Chem.* **1998**, *36*, 2637.
18. Hayes, C. O.; Chen, P. H.; Thedford, R.; Ellison, C. J.; Dong, G.; Willson, C. *Macromolecules*. **2016**, *49*, 3706.
19. Wei, Z. J.; Xu, Y. W.; Zhang, L.; Luo, M. M. *Chem. Lett.* **2014**, *25*, 1367.
20. Gies, A. P.; Spencer, L.; Rau, N. J.; Boopalachandran, P.; Rickard, M. A.; Kearns, K. L.; McDougal, N. T. *Macromolecules*. **2017**, *50*, 2304.
21. Yang, J.; Liu, S.; Zhu, F.; Huang, Y.; Li, B.; Zhang, L. *J. Polym. Sci., Part A: Polym. Chem.* **2015**, *49*, 381.
22. Yang, J.; Cheng, Y.; Xiao, F. *Eur. Polym. J.* **2012**, *48*, 751.
23. Farona, M. F. *Prog. Polym. Sci.* **1996**, *21*, 505.
24. Cheng, Y.; Tian, S.; Shi, Y.; Chen, W.; Li, Z.; Zhu, T.; Zhang, Z. *Eur. Polym. J.* **2017**, *95*, 440.
25. Cheng, Y.; Kong, L.; Ren, Z.; Qi, T. *High Perform. Polym.* **2013**, *25*, 980.
26. Yang, L.; Cao, K.; Huang, Y.; Chang, G.; Zhu, F.; Yang, J. *High Perform. Polym.* **2014**, *26*, 463.
27. Tian, S.; Sun, J.; Jin, K.; Wang, J.; He, F.; Zheng, S.; Fang, Q. *ACS Appl. Mater. Inter.* **2014**, *6*, 20437.
28. Wang, J.; Lu, C.; Liu, Y.; Wang, C.; Chu, F. *Ind. Crop Prod.* **2018**, *124*, 244.
29. Yu, J.; Liu, Y.; Liu, X.; Wang, C.; Wang, J.; Chu, F.; Tang, C. *Green Chem.* **2014**, *16*, 1854.
30. Yan, X.; Zhai, Z.; Song, Z.; Shang, S.; Rao, X. *Ind. Crop Prod.* **2017**, *108*, 371.
31. Lu, C.; Yu, J.; Wang, C.; Wang, J.; Chu, F. *Carbohydr. Polym.* **2018**, *188*, 128.
32. Li, Q.; Huang, X.; Liu, H.; Shang, S.; Song, Z.; Song, J. *ACS Sustainable Chem. Eng.* **2017**, *5*, 10002.
33. He, F.; Jin, K.; Wang, Y.; Wang, J.; Zhou, J.; Sun, J.; Fang, Q. *ACS Sustainable Chem. Eng.* **2017**, *5*, 2578.
34. Zhang, H.; Huang, X.; Jiang, J.; Shang, S.; Song, Z. *RSC Adv.* **2017**, *7*, 42541.
35. Zhang, D.; Zhou, D.; Wei, X.; Liang, J.; Chen, X.; Wang, L. *J. Supercrit. Fluids.* **2017**, *125*, 12.
36. Yang, X.; Li, Q.; Li, Z.; Xu, X.; Liu, H.; Shang, S.; Song, Z. *ACS Sustainable Chem. Eng.* **2019**, *7*, 4964.
37. Singh, V.; Joshi, S.; Malviya, T. *Int. J. Biol. Macromol.* **2018**, *112*, 390.
38. Carbonell-Blasco, P. *Int. J. Adhes. Adhes.* **2013**, *42*, 11.
39. Liu, B.; Nie, J.; He, Y. *Int. J. Adhes. Adhes.* **2016**, *66*, 99.
40. El-Ghazawy, R. A.; El-Saeed, A. M.; Al-Shafey, H. I.; Abdul-Raheim, A. M.; El-Sockary, M. A. *Eur. Polym. J.* **2015**, *69*, 403.
41. Huang, K.; Zhang, J.; Li, M.; Xia, J.; Zhou, Y. *Ind. Crop Prod.* **2013**, *49*, 497.
42. Wang, H.; Liu, X.; Liu, B.; Zhang, J.; Xian, M. *Polym. Int.* **2009**, *58*, 1435.
43. Wang, H.; Wang, H.; Zhou, G. *Polym. Int.* **2011**, *60*, 557.
44. Xu, X.; Song, Z.; Shang, S.; Cui, S.; Rao, X. *Polym. Int.* **2011**, *60*, 1521.
45. Liu, G.; Wu, G.; Chen, J.; Kong, Z. *Prog. Org. Coat.* **2016**, *101*, 461.
46. Kong, L.; Cheng, Y.; Jin, Y.; Ren, Z.; Li, Y.; Xiao, F. *J. Mater. Chem. C.* **2015**, *3*, 3364.
47. Wang, Y.; Sun, J.; Jin, K.; Wang, J.; Yuan, C.; Tong, J.; Diao, S.; He, F.; Fang, Q. *RSC Adv.* **2014**, *4*, 39884.
48. Ma, Q.; Liu, X.; Zhang, R.; Zhu, J.; Jiang, Y. *Green Chem.* **2013**, *15*, 1300.
49. He, F.; Yuan, C.; Li, K.; Diao, S.; Jin, K.; Wang, J.; Tong, J.; Ma, J.; Fang, Q. *RSC Adv.* **2013**, *3*, 23128.
50. Wan, J.; Zhao, J.; Gan, B.; Li, C.; Molina-Aldareguia, J.; Zhao, Y.; Pan, Y. T.; Wang, D. Y. *ACS Sustainable Chem. Eng.* **2016**, *4*, 2869.
51. Hardimana, M.; Vaughanb, T. J.; McCarthy, C. T. *Compos. Struct.* **2017**, *180*, 782.
52. Vanlandingham, M. R.; Villarrubia, J. S.; Guthrie, W. F.; Meyers, G. F. *Macromol. Symp.* **2001**, *167*, 15.
53. Ohba, K. *J. Photopolym. Sci. Tec.* **2002**, *15*, 177.
54. Niu, X.; Liu, Y.; Song, Y.; Han, J.; Pan, H. *Carbohydr. Polym.* **2018**, *183*, 102.
55. Fang, T.; Shimp, D. A. *Prog. Polym. Sci.* **1995**, *20*, 61.